A strategy for tissue self-organization that is robust to cellular heterogeneity and plasticity

Alec E. Cerchiari[a,b,c], James C. Garbe[b,d], Noel Y. Jee[c], Michael E. Todhunter[c], Kyle E. Broaders[c], Donna M. Peehl[e], Tejal A. Desai[a,b], Mark A. LaBarge[d], Matthew Thomson[f], and Zev J. Gartner[a,c,f,1]

[a]University of California at Berkeley–University of California at San Francisco Graduate Program in Bioengineering, University of California, Berkeley, CA 94720; Departments of [b]Bioengineering and Therapeutic Sciences and [c]Pharmaceutical Chemistry, and [f]Center for Systems and Synthetic Biology, University of California, San Francisco, CA 94143; [d]Life Sciences Division, Lawrence Berkeley National Laboratory, Berkeley, CA 94720; and [e]Stanford University School of Medicine, Stanford University, Palo Alto, CA 94305

Edited* by Ken A. Dill, Stony Brook University, Stony Brook, NY, and approved December 30, 2014 (received for review June 9, 2014)

Developing tissues contain motile populations of cells that can self-organize into spatially ordered tissues based on differences in their interfacial surface energies. However, it is unclear how self-organization by this mechanism remains robust when interfacial energies become heterogeneous in either time or space. The ducts and acini of the human mammary gland are prototypical heterogeneous and dynamic tissues comprising two concentrically arranged cell types. To investigate the consequences of cellular heterogeneity and plasticity on cell positioning in the mammary gland, we reconstituted its self-organization from aggregates of primary cells in vitro. We find that self-organization is dominated by the interfacial energy of the tissue–ECM boundary, rather than by differential homo- and heterotypic energies of cell–cell interaction. Surprisingly, interactions with the tissue–ECM boundary are binary, in that only one cell type interacts appreciably with the boundary. Using mathematical modeling and cell-type-specific knockdown of key regulators of cell–cell cohesion, we show that this strategy of self-organization is robust to severe perturbations affecting cell–cell contact formation. We also find that this mechanism of self-organization is conserved in the human prostate. Therefore, a binary interfacial interaction with the tissue boundary provides a flexible and generalizable strategy for forming and maintaining the structure of two-component tissues that exhibit abundant heterogeneity and plasticity. Our model also predicts that mutations affecting binary cell–ECM interactions are catastrophic and could contribute to loss of tissue architecture in diseases such as breast cancer.

heterogeneity | cell sorting | differential adhesion | mammary | prostate

Self-organization is a process that contributes to pattern formation and repair at all scales of biological complexity. At the tissue scale, defining robust strategies of self-organization is critical for engineering functional tissues, as well as for understanding development and the breakdown of tissue structure during diseases such as cancer (1). During development, two or more populations of motile cells can self-organize into spatially ordered tissues by a process referred to as cell sorting (2–4). The outcome of cell sorting can be rationalized using physical models that invoke cell-type-specific differences in interfacial energies. Interfacial energies arise through the action of a contractile cell cortex coupled to adhesion molecules (e.g., cadherins) that link the cortices of neighboring cells and signal to modulate cortical tension at specific cellular interfaces (5). In general, the organization of a tissue after cell sorting corresponds to a configuration that maximizes the formation of the most energetically favorable (hereafter referred to as most cell–cell cohesive)[†] cellular interfaces (6). For example, with an intermediate level of heterotypic cell–cell cohesion the most self-cohesive cell type is typically found in the tissue core, with the less cohesive cell type spread around the tissue surface (Fig. 1*A*). In order for self-organization to proceed robustly by this strategy, a tissue requires and must maintain a clearly delineated hierarchy of homo- and heterotypic cell–cell cohesive interactions.

Regulated differences in cell–cell cohesion are also thought to contribute to the self-organization and repair of adult human secretory organs such as the mammary gland (7, 8). The mammary gland, along with the prostate, salivary, lacrimal, and sweat glands, has an architecture comprising two concentrically arranged epithelial cell types as shown in Fig. 1*A*. However, the cells in the mammary gland dynamically regulate their cohesivity and motility to serve specialized roles at different locations and at different times. For example, the inner luminal (LEP) and outer myoepithelial (MEP) cells are known to undergo physical and chemical changes throughout development, menstrual cycles, pregnancy, involution, and the early stages of malignant disease. However, experiments using the mouse as a model system indicate that at the terminal end bud, where the lumen is filled and cell motility and rearrangements are elevated, cell positioning is rarely lost (9, 10). Moreover, deletion of key cell–cell adhesion proteins such as E- and P-cadherin has no gross effect on MEP or LEP cell positioning in the developing mouse mammary gland (11, 12). This is surprising given the established role of cadherins in guiding cell positioning through cell sorting. How self-organization remains robust to such severe changes to cell–cell cohesion remains unclear.

Significance

Differences in cell–cell interfacial energies can explain how multiple cell types sort into spatially organized tissues. However, this strategy of self-organization is not robust to heterogeneity or changes to the interfacial energies that drive correct cell positioning. Therefore, heterogeneous epithelial tissues such as the human mammary and prostate glands use a different strategy. First, disorganized aggregates form an adhesive interface at the tissue–ECM boundary that provides geometric constraints to self-organization. Second, only one cell type interacts appreciably with this interface. This strategy can explain how self-organization remains robust in vivo, provides generalizable rules for reconstituting tissues in vitro, and suggests how structure might break down during cancer progression.

Author contributions: A.E.C., J.C.G., D.M.P., T.A.D., M.A.L., M.T., and Z.J.G. designed research; A.E.C., J.C.G., N.Y.J., M.E.T., and K.E.B. performed research; D.M.P., T.A.D., M.A.L., and M.T. contributed new reagents/analytic tools; A.E.C. and Z.J.G. developed the biophysical assays and model; M.T. performed mathematical and computational analysis; A.E.C., M.T., and Z.J.G. analyzed data; and A.E.C., M.A.L., M.T., and Z.J.G. wrote the paper.

The authors declare no conflict of interest.

*This Direct Submission article had a prearranged editor.

[1]To whom correspondence should be addressed. Email: zev.gartner@ucsf.edu.

This article contains supporting information online at www.pnas.org/lookup/suppl/doi:10.1073/pnas.1410776112/-/DCSupplemental.

[†]We use the term "cell–cell cohesion" to capture the relative change in surface energy upon forming a cell–cell contact from dissociated cells. We use "cell–ECM cohesion" to capture the relative change in surface energy upon forming a cell–ECM contact from a dissociated cell. We use the term "cohesion" instead of "adhesion" to avoid confusing the contribution of cortical tension and adhesion tension to the process of cell–cell and cell–ECM contact formation.

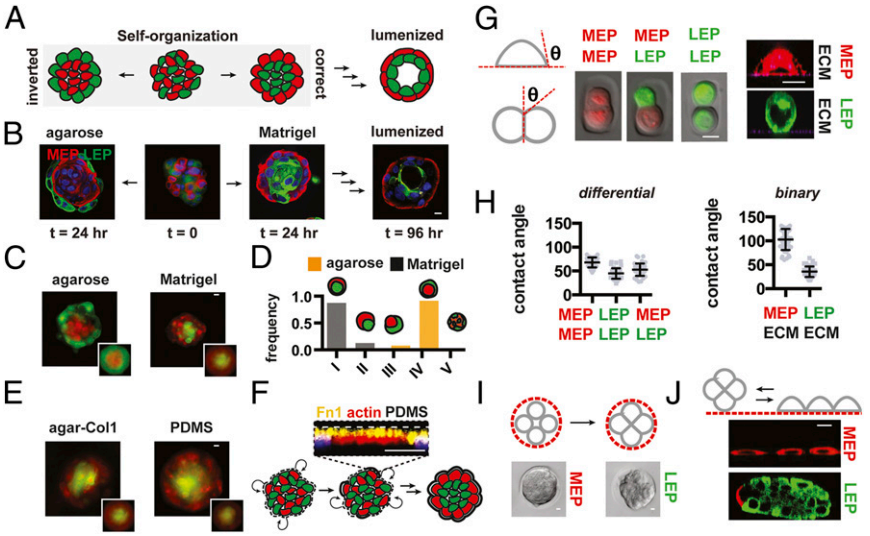

Fig. 1. A self-generated and binary adhesive interaction directs cell positioning in the mammary epithelium. (*A*) Self-organization of two initially disordered populations of cells (*Center*) into spatially ordered tissues. In the mammary gland, the correct architecture (*Right*) can go on to polarize and form a lumen. (*B*) Self-organization of fourth-passage primary human mammary epithelial cells in agarose (*Left*) and Matrigel (*Right*) after 24 h. In Matrigel, the reconstituted microtissue can also polarize and form a lumen over an additional 72 h (MEP, red, keratin-14/K14; LEP, green, keratin-19/K19; blue, DAPI/nuclei). (*C*) Experiments as in *B* but with MEP and LEP stained before self-organization with CellTracker Red (CTR) and CellTracker Green (CTG), respectively. (*Insets*) Average intensity profiles under each condition ($n = 30$). (*D*) Frequency of indicated tissue architectures for experiments in *C* ($n > 235$). (*E*) Representative images and average intensity plots of CellTracker-labeled MEP and LEP self-organized in Col1-functionalized agarose ($n = 30$) and unfunctionalized PDMS microwells ($n = 20$). (*F*) Conceptual model for self-organization by a self-generated adhesive interaction at the tissue–ECM boundary. (*Inset*) An image of MEP on an unfunctionalized PDMS surface (dotted line, PDMS; yellow, fibronectin-1; red, actin; blue, nuclei). (*G*) Representative images of cell doublets and XZ sections of single cells after 4 h on Matrigel-coated substrate (green, CTG; red, CTR; purple, QD605). (*H*) Distribution of measured contact angles at all interfaces ($n > 42$). (*I*) Representative images of aggregates of homogeneous MEP and LEP after 12 h in agarose wells. (*J*) Aggregates prepared as in *G* but subsequently transferred to Matrigel-coated glass for 12 h (green, K19; red, K14). Error bars are SD. (Scale bars, 10 μm.)

Adult tissues also comprise populations of cells that can be heterogeneous in their molecular and physical properties (13), and the mammary gland is a prototypical example of a heterogeneous tissue, possessing considerable spatial and temporal variability within both the inner luminal and outer myoepithelial populations. For example, neighboring cells in healthy tissue can differ markedly with respect to their expression of adhesion molecules, cytoskeletal proteins, hormone receptors, and the activation of specific signaling pathways (14–17). Such heterogeneity can affect the distribution of cell–cell cohesive properties among different cell types, thus confounding the ordered hierarchy of interactions necessary to drive self-organization robustly (6). Nevertheless, normal levels of tissue heterogeneity do not affect cell positioning in the gland. Even when heterogeneity in cell–cell cohesion is artificially elevated by mosaic deletion of E-cadherin, LEP and MEP retain their relative positions efficiently (18). How self-organization remains robust among these and other heterogeneous populations of cells is poorly understood.

The robustness exhibited by the mammary gland during self-organization could derive from a variety of mechanisms, including the action of intercellular regulatory networks or microenvironmental cues that fine-tune cell–cell cohesion. Here, we investigate the hypothesis that spatially restricted interfacial interactions unique to the tissue–ECM boundary are sufficient to direct robust self-organization, even among heterogeneous or changing populations of cells. To test this hypothesis, we reconstitute the self-organization of the mammary and prostate glands in vitro from aggregates of primary human cells. We then estimate the hierarchy of cell–cell and cell–ECM cohesive energies in the mammary gland to reveal that only the MEP, and not the LEP cells, adhere and spread onto the tissue–ECM boundary. Using mathematical modeling and cell-type-specific knockdown of key adhesion proteins, we show that binary (i.e., MEP adhere and LEP do not) cell–ECM cohesion dominates self-organization and is robust to changes to the hierarchy of cell–cell cohesive interactions. Our results provide a conceptual framework for understanding robust tissue formation in vivo and in vitro but also suggest several potential mechanisms through which tissue structure might break down during the progression of malignant disease.

Results

Human Mammary Epithelial Cells Can Self-Organize into an Inverted Architecture in the Absence of ECM. During self-organization, cells can interact with each other and the surrounding microenvironment to guide their ultimate position in the tissue (19). To define the relative contributions of cell–cell and cell–microenvironmental interactions on cell positioning in the mammary gland we reconstituted aggregates of human mammary epithelial cells in the presence and absence of Matrigel, a complex mixture of basement membrane proteins and growth factors that support the self-organization of numerous tissues in vitro. We used luminal (LEP; Muc1+ and Calla−) and myoepithelial cells (MEP; Muc1− and Calla+) isolated from fourth-passage cultures of human reduction mammoplasty tissue (*SI Appendix*). These purified populations of cultured primary cells were reconstituted by chemical or mechanical means at 50:50 ratios, either fully embedded within Matrigel or in nonfouling microwells (agarose) (Fig. 1*B* and *SI Appendix*) (20). Consistent with their ability to self-organize, LEP and MEP efficiently formed the correct architecture in Matrigel after 12–24 h (Movie S1). Many tissues went on to polarize and form lumens after an additional 72 h, indicating that these fourth-passage primary cells retained a complete program of self-organization including cell sorting and subsequent morphogenesis (Fig. 1*B*, *Far Right* and *SI Appendix*). Strikingly, however, these same cells also efficiently self-organized in agarose, but into a perfectly inverted architecture (Fig. 1*B*, *Left*). In this inverted architecture LEP were positioned at the tissue periphery, with MEP forming a tight aggregate in the tissue core (Movie S2). These changes in tissue architecture could not be attributed to differentiation, because identical results were observed with LEP and MEP stained with live-cell tracking dyes before reconstitution (Fig. 1 *C* and *D*). Therefore, the chemical or physical properties of Matrigel can quantitatively convert an inverted tissue configuration into one with the correct topology.

Matrigel Provides a Substrate for the Assembly of a Self-Generated Adhesive Cue at the Tissue–ECM Boundary. Matrigel could alter the outcome of self-organization by presenting specific diffusible or nondiffusible signals that alter cell–cell interactions, or by specifically modulating the tissue's interfacial energy at the tissue–ECM boundary. To exclude the possibility that Matrigel provides

specific diffusible factors or ECM components to the tissue, we repeated the self-organization assay in microwells covalently functionalized with purified ECM proteins—collagen-1 (Col1) or fibronectin-1 (Fn1)—that are only minor constituents of Matrigel (21). Both Col1- or Fn1-functionalized agarose of several concentrations effectively directed MEP from the tissue core to the periphery (Fig. 1*E* and *SI Appendix*). These results suggest that specific factors present in Matrigel are not primarily responsible for directing cell positioning. Moreover, Col1 and Fn1 were not themselves necessary to drive MEP to the tissue boundary, because we also observed correct cell positioning in polydimethylsiloxane (PDMS) microwells, a nonbiological substrate that physisorbs secreted basement membrane proteins such as Fn1 (Fig. 1*F* and *SI Appendix*). In contrast, other nonbiological but nonfouling hydrogels such as PEG-acrylate or polyacrylamide did not direct MEP to the tissue boundary. Together with the observation that basement membrane components such as laminin-5 were deposited at the MEP–Matrigel interface (*SI Appendix*), we conclude that Matrigel, PDMS, and functionalized agarose act to reorganize tissue architecture by providing an interface at the tissue boundary where cells can deposit and assemble their own adhesive basement membrane.

Cell–ECM Cohesion Is Binary Because Only MEP Interact Appreciably with the Tissue–ECM Boundary. The observation that the tissue–ECM boundary provides an additional and energetically favorable interface driving tissue self-organization prompted us to estimate the energy of cell–cell and cell–ECM cohesion for mammary epithelial cells. To do so, we compared the contact angle formed at cell–cell interfaces to the contact angles formed at the cell–ECM interface for all combinations of MEP, LEP, and a Matrigel-coated substrate. Contact angles can be related to the balance of forces at the cell–cell, cell–medium, and cell–substrate interfaces by Young's equation (*SI Appendix*). In conjunction with some simplifying assumptions and estimates of interfacial surface area, contact angle therefore provides a means of approximating the change in surface energy upon cell-contact formation for all components of the mammary epithelium. In this assay, we reproducibly found that MEP formed the most energetically favorable cell–cell interactions, having the largest cell–cell interface as well as the largest contact angle (69°; Fig. 1 *G* and *H*). This was followed by heterotypic MEP–LEP interactions (53°) and finally homotypic LEP–LEP interactions (45°). Encouragingly, these measures of cell–cell cohesion were consistent with the observation that MEP organize in the tissue core in agarose, where the most cell–cell cohesive population would maximize their homotypic interfaces.

We next measured the contact angle between LEP, MEP, and a Matrigel-coated substrate. The cell–ECM contact angle for MEP was pronounced at 4 h (Fig. 1 *G* and *H*) and converged to a value of 119° after an additional 8 h (*SI Appendix*). Strikingly, however, the vast majority of LEP were unable to interact with the Matrigel-coated surface. Those few cells that interacted had an average contact angle near the lower limit of detection for the assay (*SI Appendix*). These properties of MEP and LEP were retained at the multicellular level, because the more cell–cell cohesive MEP aggregates had higher circularity than the less cell–cell cohesive LEP aggregates yet preferentially spread on ECM-coated surfaces (Fig. 1 *I* and *J* and *SI Appendix*). Cell–ECM cohesive differences between MEP and LEP were also reflected at the molecular level, where we found that most components of the ECM adhesion machinery, including multiple integrin subunits and basement membrane proteins, were overexpressed in MEP relative to LEP (*SI Appendix*).

Together, these measurements suggest that although homo- and heterotypic cell–cell cohesive interactions can span a spectrum of values in the mammary gland and are capable of directing self-organization independent of ECM into an inverted architecture, cell–ECM cohesion at the tissue boundary is a property unique to the MEP population. Along with the observation that MEP synthesize an adhesive ECM boundary, these measurements suggest that remodeling of the tissue–ECM boundary drives tissue self-organization toward the correct in vivo architecture by providing a new interface. Strikingly, cell–ECM cohesion to this interface is binary, in that LEP–ECM cohesion is maintained at a minimum.

Spatially Restricted and Binary Cell–ECM Cohesion Need Not Be the Most Energetically Favorable Interaction to Dominate Self-Organization. In contrast to individual cell–cell interactions that span a spectrum of interaction energies and rearrange dynamically within the tissue, cell–ECM interactions are binary and spatially restricted to the outer edge of the tissue where basement membrane components accumulate. These qualitative differences between cell–cell and cell–ECM interactions could have important consequences on the robustness of self-organization. We therefore implemented a coarse-grained and lattice-based mathematical model to compare the relative stability of the correct and inverted architectures as a function of the geometry and the relative stability of each type of cell–cell and cell–ECM interaction (Fig. 2 *A* and *B* and *SI Appendix*). In this model, we treated ECM as a set of static cells that define the tissue boundary. We calculated that a phase transition between the inverted and correct tissue architectures would occur when the energy of MEP–ECM cohesion ($W_{MEP\text{-}ECM}$) satisfies the following inequality:

$$W_{MEP-ECM} > (W_{MEP-MEP} - W_{LEP-LEP}) * \varnothing(r) + W_{LEP-ECM}$$

where $\varnothing(r)$ is a geometric parameter (*SI Appendix*). How strong must $W_{MEP\text{-}ECM}$ be to dominate self-organization under conditions of binary cell–ECM cohesion? To answer this question, we calculated the minimum interaction energy between MEP and ECM necessary to correct an inverted architecture given the energies of interaction estimated for the other components of the tissue (Fig. 2*A* and *SI Appendix*). We found that the correct tissue architecture is favored when $W_{MEP-ECM}$ is greater than 2.5-fold $W_{LEP-LEP}$, the weakest of the cell–cell cohesive interactions. Surprisingly, this value of $W_{MEP-ECM}$ is less than the magnitude of both $W_{MEP-MEP}$ and $W_{MEP-LEP}$ in the model. Therefore, this analysis highlights the importance of a spatially restricted adhesive cue on self-organization. It also highlights the importance of on-or-off (i.e., binary because $W_{LEP-ECM} = 0$) cell–ECM cohesion because the strength of $W_{MEP-ECM}$ necessary to correct an inverted architecture increases directly with the strength of $W_{LEP-ECM}$.

Binary Cell–ECM Cohesion Sustains Self-Organization upon Perturbation to Cell–Cell Cohesion. To explore the robustness of self-organization to varied parameters mimicking plasticity in cell–cell cohesion, we implemented the mathematical model computationally. We first confirmed that the computational model converged on the correct and inverted tissue architecture in the presence or absence of an adhesive tissue boundary, respectively (Fig. 2*B* and *SI Appendix*). We then tested combinations of parameters for cell–cell interactions across 10,000 runs of the model and plotted the results of each run as a sphere on a 3D phase diagram. Each sphere's color corresponds to distinct tissue configurations (Fig. 2*C*). In the presence of binary cell–ECM cohesion, we found that the correct configuration (red sphere) was stable across the majority of sampled parameters. In contrast, tissue configuration was exquisitely sensitive to changes to the hierarchy of cell–cell cohesive interactions in the absence of binary cell–ECM cohesion. Indeed, the tissue seemed poised near numerous phase boundaries such that small perturbations to parameters triggered large-scale transitions between dissimilar tissue architectures in the model.

More detailed visual analysis of the phase diagram suggested several testable hypotheses (Fig. 2*D*). First, tissue self-organization

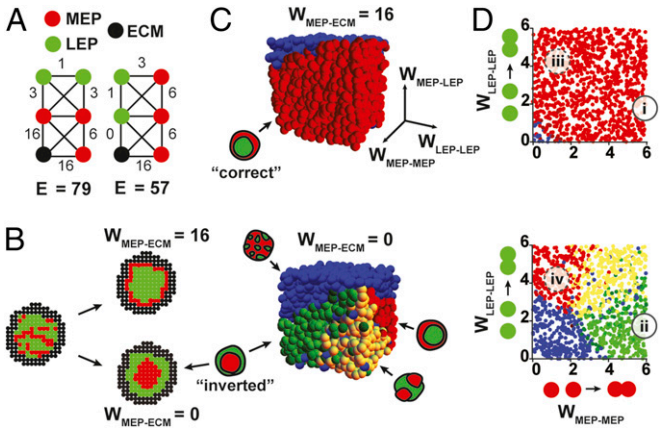

Fig. 2. A lattice-based model of self-organization predicts robustness to perturbations affecting cell–cell cohesion in the presence of an adhesive tissue boundary. (*A*) Two configurations of LEP (green), MEP (red), and ECM (black) with different stabilities. Numbers on edges represent the strength (relative to LEP–LEP) of specific interactions. Larger numbers represent more favorable interactions. (*B*) Output of Monte-Carlo simulations using the indicated values for $W_{MEP-ECM}$ for tissue self-organization on a square lattice with stationary ECM. (*C*) Phase diagrams for tissue self-organization in the presence (*Top*) and absence (*Bottom*) of MEP–ECM interactions. Each sphere represents a single run of the model. Color represents the given tissue architecture (small icons). (*D*) Cross-sections through the phase diagrams in *C* reveal the combinations of parameters representative of fourth-passage human primary mammary epithelial cells in the presence of ECM (i). Positions ii–iv represent predicted tissue phases upon specific perturbations described in the text.

should be robust to pronounced decreases of MEP–MEP or LEP–LEP cohesion in the presence of an adhesive ECM boundary (e.g., perturbation i → iii). In contrast, the same perturbations should lead to a transition between dissimilar tissue configurations in the absence of an adhesive tissue boundary (e.g., perturbation ii → iv). To measure the impact of perturbations to cell–cell cohesion on self-organization, we used siRNA to knock down p120 catenin in the most cell–cell cohesive MEP population. p120 catenin is necessary for stabilizing cadherin-mediated cell–cell interfaces and, as expected, knockdown of p120 catenin caused a dramatic reduction in MEP–MEP cohesion as determined by a decrease in contact angle and a reduction in aggregate circularity (Fig. 3 *A* and *B* and *SI Appendix*). However, p120 knockdown did not have a significant effect on cell–ECM contact angle over a similar timeframe (Fig. 3*C* and *SI Appendix*). To assay for self-organization, we forced aggregation of control LEP with p120 knockdown MEP by either mechanical or chemical means (*SI Appendix*) (22–24). Consistent with the predictions of the model, we observed a transition among tissue architectures in nonadhesive agarose: Instead of an inverted tissue architecture, the now less-cohesive MEP moved to the periphery of the tissue, allowing the control LEP to maximize their interactions at the tissue core (Fig. 3*D*). However, the decrease in MEP–MEP cohesion did not alter the outcome of self-organization in Matrigel, where control LEP remained in the tissue core and p120 knockdown MEP spread at the tissue–ECM boundary (Fig. 3 *E* and *F*).

The computational model also predicted that a loss of cell–ECM cohesion in the MEP population should be sufficient to trigger a transition toward the inverted architecture, independent of the physical or chemical properties of the surrounding matrix. However, we found that knockdown of single integrins such as β1 in MEP did not efficiently block cell spreading on complex ECM such as Matrigel, and thus did not significantly affect self-organization (*SI Appendix*). This observation can be explained by the redundant expression of multiple integrins by MEP but also suggests an important role for cortical tension in MEP spreading on ECM, as well as self-organization. We therefore knocked down Talin1—an adapter protein necessary for linking the contractile actomyosin cytoskeleton to integrins (25)—and observed a significant reduction in MEP–ECM contact angle and the spreading of multicellular aggregates on Matrigel-coated substrates (Fig. 3 *A* and *C* and *SI Appendix*). Talin1 knockdown did not appear to perturb MEP–MEP cohesion as measured by cell–cell contact angle at 4 h (Fig. 3*B*), although we did observe a reduction in MEP aggregate circularity after 12 h (26). Consistent with their cell–cell and cell–ECM cohesion phenotypes, Talin1 knockdown MEP reconstituted with control LEP assembled efficiently into the inverted architecture in agarose (Fig. 3*G*) but were unable to efficiently self-organize into the correct architecture in Matrigel (Fig. 3 *H* and *I*). Taken together, these experiments indicate that, in the presence of an adhesive tissue–ECM boundary, binary cell–ECM cohesion can direct cell positioning even upon dramatic perturbations to cell–cell cohesion.

Self-Organization of the Mammary Gland Is Robust to Highly Variable Cell–Cell Interactions. We also tested how binary cell–ECM cohesion could moderate the effects of highly variable cell–cell cohesion on tissue self-organization. To do so, we used uncultured primary cells isolated from human reduction mammoplasty tissue. Compared with the fourth-passage primary cells used in our previous experiments, uncultured primary cells have elevated levels of cellular heterogeneity in a variety of cell-surface markers (15, 27). Consistent with underlying variability in the energetics of their cellular interfaces, we found that pure populations of uncultured luminal or myoepithelial cells formed aggregates with more variable and overlapping circularity than fourth-passage primary cells (Fig. 4*A*). However, these uncultured primary cells retained

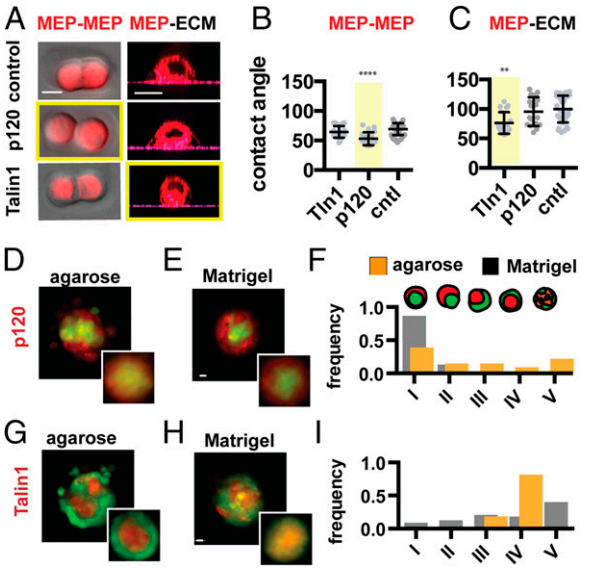

Fig. 3. Self-organization is robust to perturbation of cell–cell cohesion only in the presence of an adhesive tissue boundary. (*A*) Representative images of MEP used to measure contact angles at the cell–cell and cell–ECM interfaces for the given perturbations. (*B*) Quantification of MEP contact angles (and SD) at the cell–cell and (*C*) cell–ECM interfaces (n = 16–56) for the given perturbations. Measurements for Talin1 knockdown cells do not account for a significant fraction of the population that do not adhere to matrix and are removed during wash steps. (*D*) Representative image and average intensity plots (*Inset*, n = 20) for p120 knockdown MEP self-organized with control LEP in agarose and (*E*) Matrigel. (*F*) Distributions of tissue architectures from *D* and *E* (n = 45–54). (*G*) Representative image and average intensity profiles (*Inset*, n = 20) for Talin1 knockdown MEP with control LEP in agarose and (*H*) Matrigel. (*I*) Distributions of tissue architectures from *G* and *H* (n = 72–81). Red, CellTracker Red; green, CellTracker Green. (Scale bars, 10 μm.)

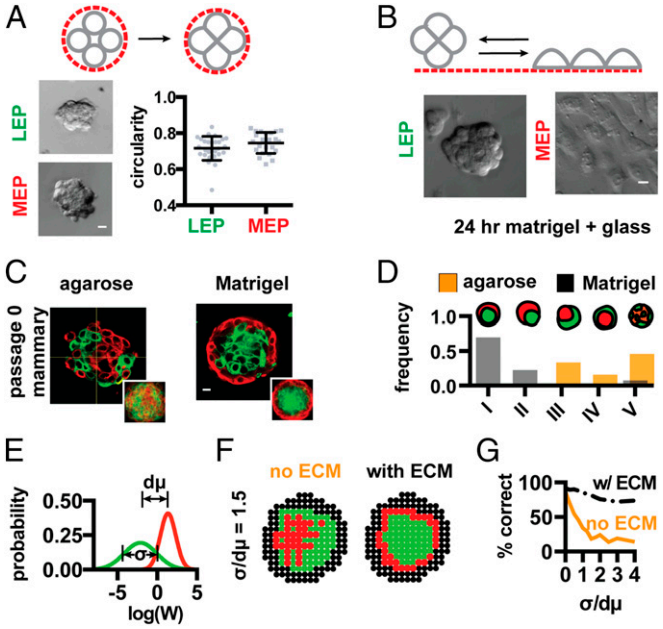

Fig. 4. An adhesive tissue boundary supports self-organization among populations of cells that are heterogeneous in their cohesive properties. (*A*) Circularity of pure aggregates of uncultured human primary mammary LEP and MEP ($n > 23$). (*B*) Aggregate spreading assay of pure uncultured LEP and MEP. (*C*) Representative images and average keratin intensity profiles (*Inset*, $n = 20$) for uncultured primary human mammary epithelial cells self-organizing in agarose (*Left*) and Matrigel (*Right*). Red, K14; green, K19. (*D*) Distribution of tissue architectures for self-organizing uncultured primary cells in Matrigel (gray, $n = 53$) and agarose (orange, $n = 56$). (*E*) Log-normal homotypic interaction energy distributions for LEP (green) and MEP (red) ($\sigma/d\mu = 1.5$). (*F*) Simulated self-organization of LEP (green) and MEP (red) in agarose (*Left*) and Matrigel (*Right*), but with $\sigma/d\mu = 1.5$. (*G*) The relative efficiency of self-organization to an identical tissue architecture (configuration I) as a function of cell-to-cell variability using a strategy of binary cell–ECM adhesion (black; $W_{MEP\text{–}ECM} = 2 \times W_{MEP\text{–}MEP}$) or differential cell–cell cohesion alone (orange). (Scale bars, 10 μm.)

their strong and binary cell–ECM cohesive properties as judged by aggregate spreading assays (Fig. 4*B*). Therefore, it was not surprising that these heterogeneous uncultured primary cells could not self-organize robustly in agarose but could still form the correct architecture in Matrigel (Fig. 4 *C* and *D* and *SI Appendix*). These results were generalizable to another tissue sharing the architecture of the mammary gland: the human prostate. Populations of uncultured and healthy basal and luminal cells isolated from human prostatectomies were found to self-organize efficiently in Matrigel, but not in agarose (*SI Appendix*). Furthermore, we found that healthy basal prostate cells retained strong cell–ECM cohesion and self-organized robustly with cultured luminal mammary epithelial cells that lacked cell–ECM cohesion (*SI Appendix*). Therefore, the rules that guide cell positioning in the mammary and prostate are cross-compatible, and thus entirely independent of tissue-specific cell function.

To test the extent to which a binary adhesive interaction with the tissue boundary renders self-organization robust to cell-to-cell variability, we revised the computation model, drawing energies of interaction for individual cells of a given cell type from a distribution of values with a characteristic standard deviation (SD), rather than from a single value as in previous cases (Fig. 4*E* and *SI Appendix*). As the SD in the energy of cell–cell interactions became large, the model produced observations qualitatively similar to those seen in Matrigel and agarose: increased variability had little impact on the correct architecture in the presence of binary cell–ECM cohesion, whereas the inverted architecture trended toward disorganization in the absence of binary cell–ECM cohesion (Fig. 4 *F* and *G*).

Discussion

The fine-tuning of multiple cell–cell cohesive interactions is believed to direct self-organization to a specific tissue architecture in a variety of biological processes. During development, changes to this balance of interactions can be used to drive tissue rearrangements and morphogenesis (28). In adult tissues, however, disrupting this balance of interactions would disrupt the capacity of multiple populations of cells to retain a single correct multicellular architecture in the absence of other mechanisms of control. Such disruptions can occur when cell populations are heterogeneous or when cellular properties must be plastic to adapt to the changing needs of a dynamic tissue environment. Using primary human mammary epithelial cells as a model system, we confirm this notion and show that self-organization through differential cell–cell cohesive interactions is sensitive to perturbation and cell-to-cell variability. To provide robustness to this process, we find that the outer myoepithelial population adheres to basement membrane components it deposits at the tissue boundary. This cell–ECM cohesive interaction is spatially restricted and binary, in that it is unique to the MEP population. Although our model does not take into account matrix mechanical properties, which can affect $W_{MEP\text{–}ECM}$ and the kinetics of self-organization (*SI Appendix*), a self-generated and binary cell–ECM interaction can drive the rapid collapse of the MEP population to the tissue edge, even when it is not the strongest interaction in the system. Although the tissue boundary is composed of ECM in the mammary and prostate glands, our model makes no assumption about its properties other than providing a spatially restricted and cohesive interface to only one cell population. Thus, the tissue boundary need not be ECM to promote robust self-organization by this general mechanism but may comprise other materials or even stationary populations of cells (2, 29, 30). Control of self-organization by the properties of the surrounding medium is conceptually analogous to protein folding, where hydrophobic collapse drives the initial stages of protein folding and is dominated by the energetics of hydrophobic and hydrophilic amino acid side-chain interactions with the aqueous solvent (31).

Our finding that cell–cell cohesion is largely dispensable in guiding MEP and LEP cell positioning in the mammary gland is surprising but consistent with several unusual observations in mouse models of glandular development. For example, ablation of key epithelial cell–cell adhesion molecules such as P- or E-cadherin during the development of the mouse mammary gland does not dramatically alter cell positioning (11, 12, 32). Even ablation of p120 catenin did not alter the relative positioning of MEP and LEP with respect to the tissue boundary, although it did trigger glandular thickening and lumen filling (33). On its surface, our finding that binary MEP–ECM cohesion dominates tissue self-organization seems inconsistent with several reports that integrins are dispensable for cell positioning during mouse mammary gland development (34). However, MEP express numerous integrins that seem to be able to partially compensate for one another in the process of self-organization. Moreover, our mathematical model predicts that MEP–ECM cohesion need not be the dominant interaction to direct cell positioning correctly so long as LEP–ECM cohesion is maintained near zero. Consistent with this notion, we found that knockdown of single integrins such as β_1 did not significantly influence tissue self-organization in Matrigel despite slightly decreasing MEP–ECM spreading (*SI Appendix*). However, perturbations affecting the ability of multiple members of the integrin family to transduce force or to assemble a contractile cytoskeleton (e.g., Talin1 KD, Latrunculin A, or Y26732; *SI Appendix*) had a more substantial effect on both MEP–ECM contact angle as well as self-organization. These findings might provide a

more physical explanation for how mammary epithelial cell spreading on ECM affects tissue architecture in vivo (35).

The dominant role of myoepithelial cells in guiding the self-organization of the mammary gland is particularly interesting in light of their hypothesized role as cellular tumor suppressors and master regulators of tissue architecture (36, 37). Luminal epithelial cells or their progenitors are widely believed to be the cell of origin in most breast cancers (38). In contrast, myoepithelial cells are rarely transformed and act as cellular tumor suppressors by decreasing proliferation and blocking access of transformed luminal cells to the ECM, where they can take on more basal characteristics and invade (39). Therefore, loss of MEP positioning is commonly associated with a transition from non-invasive to invasive breast cancer (40). Given that MEP are rarely transformed, what sorts of physical changes in the LEP population could contribute to a breakdown in robust MEP positioning? Mathematical modeling suggests at least two classes of perturbations to luminal cells that would affect myoepithelial cell positioning without specifically altering the strength of MEP interactions with the ECM or other cells. First, simply increasing LEP–ECM adhesion (i.e., loss of binary adhesion by increasing $W_{LEP-ECM}$) could have profound changes on tissue architecture. Recent studies support this notion. For example, activation of epithelial–mesenchymal transition within the mammary gland by overexpression of Twist1 triggers rapid cell dissemination and a breakdown in cell positioning within the gland. Surprisingly, expression profiling revealed that these architectural changes coincided with an up-regulation of basal adhesion machinery rather than alterations in cell–cell cohesion (18). Second, our model predicts that processes that lead to ductal swelling and lumen filling owing to aberrant luminal cell growth would decrease the tissue surface to volume ratio (e.g., changing the parameter $\varnothing(r)$; *SI Appendix*), thereby decreasing the influence of the tissue boundary on cell positioning. Supporting this notion, deletion of the proapoptotic protein BIM during mammary development was found to trigger lumen filling and terminal end bud dilation. This process coincided with the appearance of numerous cells expressing MEP markers in the tissue core (10). Although these reports are intriguing, future efforts will be needed to dissect the precise relationship between matrix physicochemical properties, cell adhesion, tissue geometry, and the capacity of LEP and MEP to form, retain, and remodel the correct architecture of the mammary gland during tumor progression.

Materials and Methods

Experimental procedures used for dissociating, purifying, transfecting, reconstituting, and culturing human mammary and prostate epithelial cells can be found in *SI Appendix*, including a discussion of analytical methods and computational experiments.

ACKNOWLEDGMENTS. The authors thank Dr. Maija Valta for help in preparing primary prostate organoids, Dr. Jennifer Liu and Dr. Alba de Moniz for technical assistance and comments, Dr. Justin Farlow for help with data analysis, and an anonymous reviewer for helpful comments on the manuscript. This work was supported by a seed grant from the National Institutes of Health (NIH) Bay Area Physical Sciences and Oncology Center (to Z.J.G. and M.A.L.); Department of Defense Breast Cancer Research Program Grants W81XWH-10-1-1023 and W81XWH-13-1-0221 (to Z.J.G.); NIH common funds Grants DP5 OD012194-03 (to M.T.) and DP2 HD080351-01 (to Z.J.G.); the Sidney Kimmel Foundation; and the University of California, San Francisco (UCSF) Program in Breakthrough Biomedical Research. Z.J.G. and M.T. are supported by the UCSF Center for Systems and Synthetic Biology (National Institute of General Medical Sciences Systems Biology Center Grant P50 GM081879). A.E.C. was supported by the US Department of Defense through a National Defense Science and Engineering Graduate Fellowship.

1. Sasai Y (2013) Cytosystems dynamics in self-organization of tissue architecture. *Nature* 493(7432):318–326.
2. Townes PL, Holtfreter J (1955) Directed movements and selective adhesion of embryonic amphibian cells. *J Exp Zool* 128(1):53–120.
3. Xiong F, et al. (2013) Specified neural progenitors sort to form sharp domains after noisy Shh signaling. *Cell* 153(3):550–561.
4. Dietrich J-E, Hiiragi T (2007) Stochastic patterning in the mouse pre-implantation embryo. *Development* 134(23):4219–4231.
5. Maître J-L, et al. (2012) Adhesion functions in cell sorting by mechanically coupling the cortices of adhering cells. *Science* 338(6104):253–256.
6. Steinberg MS (1963) Reconstruction of tissues by dissociated cells. Some morphogenetic tissue movements and the sorting out of embryonic cells may have a common explanation. *Science* 141(3579):401–408.
7. Chanson L, et al. (2011) Self-organization is a dynamic and lineage-intrinsic property of mammary epithelial cells. *Proc Natl Acad Sci USA* 108(8):3264–3269.
8. Runswick SK, O'Hare MJ, Jones L, Streuli CH, Garrod DR (2001) Desmosomal adhesion regulates epithelial morphogenesis and cell positioning. *Nat Cell Biol* 3(9):823–830.
9. Ewald AJ, Brenot A, Duong M, Chan BS, Werb Z (2008) Collective epithelial migration and cell rearrangements drive mammary branching morphogenesis. *Dev Cell* 14(4):570–581.
10. Mailleux AA, et al. (2007) BIM regulates apoptosis during mammary ductal morphogenesis, and its absence reveals alternative cell death mechanisms. *Dev Cell* 12(2):221–234.
11. Radice GL, et al. (1997) Precocious mammary gland development in P-cadherin-deficient mice. *J Cell Biol* 139(4):1025–1032.
12. Boussadia O, Kutsch S, Hierholzer A, Delmas V, Kemler R (2002) E-cadherin is a survival factor for the lactating mouse mammary gland. *Mech Dev* 115(1-2):53–62.
13. Altschuler SJ, Wu LF (2010) Cellular heterogeneity: Do differences make a difference? *Cell* 141(4):559–563.
14. Moreira JMAJ, et al. (2010) Tissue proteomics of the human mammary gland: Towards an abridged definition of the molecular phenotypes underlying epithelial normalcy. *Mol Oncol* 4(6):539–561.
15. Keller PJ, et al. (2010) Mapping the cellular and molecular heterogeneity of normal and malignant breast tissues and cultured cell lines. *Breast Cancer Res* 12(5):R87.
16. Shehata M, et al. (2012) Phenotypic and functional characterisation of the luminal cell hierarchy of the mammary gland. *Breast Cancer Res* 14(5):R134.
17. Bloushtain-Qimron N, et al. (2008) Cell type-specific DNA methylation patterns in the human breast. *Proc Natl Acad Sci USA* 105(37):14076–14081.
18. Shamir ER, et al. (2014) Twist1-induced dissemination preserves epithelial identity and requires E-cadherin. *J Cell Biol* 204(5):839–856.
19. Bissell MJ, Hall HG, Parry G (1982) How does the extracellular matrix direct gene expression? *J Theor Biol* 99(1):31–68.
20. Cerchiari A, et al. (2014) Formation of spatially and geometrically controlled three-dimensional tissues in soft gels by sacrificial micromolding. *Tissue Eng Part C Methods*, in press.
21. Kleinman HK, et al. (1986) Basement membrane complexes with biological activity. *Biochemistry* 25(2):312–318.
22. Liu JS, Farlow JT, Paulson AK, Labarge MA, Gartner ZJ (2012) Programmed cell-to-cell variability in Ras activity triggers emergent behaviors during mammary epithelial morphogenesis. *Cell Reports* 2(5):1461–1470.
23. Selden NS, et al. (2012) Chemically programmed cell adhesion with membrane-anchored oligonucleotides. *J Am Chem Soc* 134(2):765–768.
24. Gartner ZJ, Bertozzi CR (2009) Programmed assembly of 3-dimensional microtissues with defined cellular connectivity. *Proc Natl Acad Sci USA* 106(12):4606–4610.
25. Zhang X, et al. (2008) Talin depletion reveals independence of initial cell spreading from integrin activation and traction. *Nat Cell Biol* 10(9):1062–1068.
26. Robinson EE, Zazzali KM, Corbett SA, Foty RA (2003) Alpha5beta1 integrin mediates strong tissue cohesion. *J Cell Sci* 116(Pt 2):377–386.
27. Garbe JC, et al. (2012) Accumulation of multipotent progenitors with a basal differentiation bias during aging of human mammary epithelia. *Cancer Res* 72(14):3687–3701.
28. Ohnishi Y, et al. (2014) Cell-to-cell expression variability followed by signal reinforcement progressively segregates early mouse lineages. *Nat Cell Biol* 16(1):27–37.
29. Krieg M, et al. (2008) Tensile forces govern germ-layer organization in zebrafish. *Nat Cell Biol* 10(4):429–436.
30. Keller R, Davidson LA, Shook DR (2003) How we are shaped: The biomechanics of gastrulation. *Differentiation* 71(3):171–205.
31. Dill KA, et al. (1995) Principles of protein folding—a perspective from simple exact models. *Protein Sci* 4(4):561–602.
32. Evers B, et al. (2010) A tissue reconstitution model to study cancer cell-intrinsic and -extrinsic factors in mammary tumourigenesis. *J Pathol* 220(1):34–44.
33. Kurley SJ, et al. (2012) p120-catenin is essential for terminal end bud function and mammary morphogenesis. *Development* 139(10):1754–1764.
34. Klinowska TC, et al. (2001) Epithelial development and differentiation in the mammary gland is not dependent on alpha 3 or alpha 6 integrin subunits. *Dev Biol* 233(2):449–467.
35. van Miltenburg MHAM, et al. (2009) Complete focal adhesion kinase deficiency in the mammary gland causes ductal dilation and aberrant branching morphogenesis through defects in Rho kinase-dependent cell contractility. *FASEB J* 23(10):3482–3493.
36. Adriance MC, Inman JL, Petersen OW, Bissell MJ (2005) Myoepithelial cells: Good fences make good neighbors. *Breast Cancer Res* 7(5):190–197.
37. Gudjonsson T, et al. (2002) Normal and tumor-derived myoepithelial cells differ in their ability to interact with luminal breast epithelial cells for polarity and basement membrane deposition. *J Cell Sci* 115(Pt 1):39–50.
38. Keller PJ, et al. (2012) Defining the cellular precursors to human breast cancer. *Proc Natl Acad Sci USA* 109(8):2772–2777.
39. Cheung KJ, Gabrielson E, Werb Z, Ewald AJ (2013) Collective invasion in breast cancer requires a conserved basal epithelial program. *Cell* 155(7):1639–1651.
40. Rudland PS (1991) Histochemical organization and cellular composition of ductal buds in developing human breast: Evidence of cytochemical intermediates between epithelial and myoepithelial cells. *J Histochem Cytochem* 39(11):1471–1484.